Zebrafish screen identifies novel compound with selective toxicity against leukemia

*Suzanne Ridges,[1] *Will L. Heaton,[1] *Deepa Joshi,[1] Henry Choi,[1] Anna Eiring,[1] Lance Batchelor,[1] Priya Choudhry,[1] Elizabeth J. Manos,[1] Hossein Sofla,[1] Ali Sanati,[1] Seth Welborn,[1] Archana Agarwal,[2] Gerald J. Spangrude,[2] Rodney R. Miles,[2] James E. Cox,[3] J. Kimble Frazer,[1,4] Michael Deininger,[1,5] Kaveri Balan,[6] Matthew Sigman,[6] Markus Müschen,[7] Tatiana Perova,[8,9] Radia Johnson,[8,10] Bertrand Montpellier,[8] Cynthia J. Guidos,[8-10] David A. Jones,[1] and Nikolaus S. Trede[1,4]

[1]Department of Oncological Sciences, Huntsman Cancer Institute, [2]Department of Pathology, [3]Metabolomics Core Facility, and Departments of [4]Pediatrics, [5]Hematology, and [6]Chemistry, University of Utah, Salt Lake City, UT; [7]Leukemia and Lymphoma Program, Norris Comprehensive Cancer Center, University of Southern California, Los Angeles, CA; [8]Program in Developmental and Stem Cell Biology, Hospital for Sick Children Research Institute, Toronto, ON; and Departments of [9]Medical Biophysics and [10]Immunology, University of Toronto, Toronto, ON

To detect targeted antileukemia agents we have designed a novel, high-content in vivo screen using genetically engineered, T-cell reporting zebrafish. We exploited the developmental similarities between normal and malignant T lymphoblasts to screen a small molecule library for activity against immature T cells with a simple visual readout in zebrafish larvae. After screening 26 400 molecules, we identified Lenaldekar (LDK), a compound that eliminates immature T cells in developing zebrafish without affecting the cell cycle in other cell types. LDK is well tolerated in vertebrates and induces long-term remission in adult zebrafish with cMYC-induced T-cell acute lymphoblastic leukemia (T-ALL). LDK causes dephosphorylation of members of the PI3 kinase/AKT/mTOR pathway and delays sensitive cells in late mitosis. Among human cancers, LDK selectively affects survival of hematopoietic malignancy lines and primary leukemias, including therapy-refractory B-ALL and chronic myelogenous leukemia samples, and inhibits growth of human T-ALL xenografts. This work demonstrates the utility of our method using zebrafish for antineoplastic candidate drug identification and suggests a new approach for targeted leukemia therapy. Although our efforts focused on leukemia therapy, this screening approach has broad implications as it can be translated to other cancer types involving malignant degeneration of developmentally arrested cells. (*Blood*. 2012;119(24):5621-5631)

Introduction

The yearly incidence in the US for all leukemia types, including acute lymphoblastic leukemia (ALL), acute myeloid leukemia (AML), and chronic myelogenous leukemia (CML), was estimated at more than 40 000 men and women in 2010, with a yearly death rate of 50%.[1] More than 2000 cases of ALL are diagnosed in US children every year, making it the most common childhood cancer.[2] T-cell ALL (T-ALL) represents approximately 15% and 25% of pediatric and adult ALL cases, respectively.[3] Although leukemia treatment has become increasingly efficient over the past 50 years, mortality from ALL is still 20% for children and more than 40% for adults, and T-ALL has been more difficult to treat than B-cell ALL (B-ALL).[4] Currently, research efforts are devoted to molecular-based risk stratification of patients and the development of targeted therapies to limit side effects[5-7] and to increase treatment efficacy.

Development of targeted cancer therapies typically requires knowledge of the molecular target.[8] In the absence thereof, an alternative approach may use a robust readout designed to screen large numbers of compounds for specific effects[9] against the malignant cell type in question. More than 50% of patients with T-ALL have deregulated NOTCH1,[10] and in a recent study 47% had mutations in the PI3 kinase/AKT/mTOR (P/A/mT) pathway.[11] NOTCH1 signaling requires proteolytic cleavage by γ-secretase and other proteases[12] to release the intracytoplasmic domain, providing severalpotential targets for therapeutic intervention. Targeted treatment approaches for T-ALL using γ-secretase inhibitors (GSIs), although appearing a priori promising, have been disappointing,[13] possibly through pre-existing or newly acquired mutations in phosphatase and tensin homolog (PTEN) that render many T-ALL cell lines AKT-addicted.[14] However, others found that even in the absence of PTEN, primary murine and human T-ALL samples remain sensitive to NOTCH inhibition.[15] Overall, gain-of-function mutations in the NOTCH1 and P/A/mT pathways are strongly selected for in human T-ALL. This has raised interest in clinically useful, nontoxic inhibitors of the P/A/mT pathway[13] for leukemia and other cancers,[16] and makes combined treatment approaches (anti-NOTCH, anti-P/A/mT) attractive.[17]

Small molecule screens can be carried out in vitro either using biochemical assays or cell lines. Although often successful in providing "hits," these approaches lack the biologic context of an entire vertebrate organism, and identified active compounds often fail when applied in vivo because of poor bioavailability or toxicity. Although mice are an integral component of preclinical drug development, their use for high-throughput drug screening is fiscally prohibitive. Small animal models are therefore needed. For

Submitted December 19, 2011; accepted March 11, 2012. Prepublished online as *Blood* First Edition paper, April 9, 2012; DOI 10.1182/blood-2011-12-398818.

*S.R., W.L.H., and D.J. contributed equally to this work.

There is an Inside *Blood* commentary on this article in this issue.

The online version of this article contains a data supplement.

The publication costs of this article were defrayed in part by page charge payment. Therefore, and solely to indicate this fact, this article is hereby marked "advertisement" in accordance with 18 USC section 1734.

anti–T-ALL drug development, the zebrafish (*Danio rerio*) appears particularly well-suited because its adaptive immune system is similar to that of humans,[18] T-ALL models have been established,[19,20] and its use for in vivo drug discovery is advantageous (reviewed by Langenau et al[21]).

We have previously shown that dexamethasone, widely used for treatment of T-ALL, can eliminate immature T cells from the thymus of zebrafish larvae carrying the T-cell specific *p56^{lck}-promoter*:enhanced green fluorescence protein (*lck*:EGFP) transgene.[21] In a novel zebrafish screen we searched a small molecule library for compounds that similarly eliminate immature T cells from 5 days post fertilization (dpf) *lck*:EGFP larvae, reasoning that active compounds may also eliminate developmentally arrested, immature T-ALL blasts. One compound we identified, with previously unknown biologic activity, is active against immature normal and cMYC-transformed leukemic T cells in adult zebrafish[20] and has selective activity against human leukemia lines. We named the compound Lenaldekar (LDK; 1H-indole-3-carbaldehyde 8-quinolinylhydrazone). LDK is well tolerated in mice, has favorable pharmacokinetics, and slows the in vivo growth of human T-ALL in murine xenografts. Importantly, LDK is active against primary human leukemia cells, including T315I mutated, BCR-ABL positive, therapy-refractory B-ALL and CML samples. We show that in all sensitive cells LDK has 2 independent activities: delay in late mitosis and inhibition of the P/A/mT pathway, probably by an indirect route. LDK-resistant cells tested to date lack mitotic delay, suggesting that both activities of LDK may be required for cytotoxicity and providing a possible mechanistic basis for its selectivity. We propose that LDK's unique activity offers a new, targeted approach to leukemia treatment.

Methods

Zebrafish and mouse studies

Animal studies were performed according to the University of Utah animal protocol guidelines under protocol numbers 11-07006 (zebrafish) and 09-11001 and 09-11002 (mouse).

Zebrafish drug screen

The transgenic *p56^{lck}*:EGFP zebrafish line (*lck*:EGFP) was previously described.[21] *lck*:EGFP transgenic zebrafish were bred and eggs collected and raised in E3 water 5 to 6 dpf. Larvae were then aliquoted 3 per well in a 96-well format in 300 μL E3 fish water. Compounds for screening from the ChemBridge DIVERSet Library (ChemBridge) were added to each well of the duplicate plates at a final concentration of 10μM. Zebrafish larvae were examined after 2 days of incubation in compounds and scored for thymus fluorescence via Nikon Eclipse E600 imaging system by 2 operators. Scores ("unchanged," "moderate," or "strong reduction" of fluorescence emitted from T cells in thymus compared with diluent treated controls) were compared and reconciled. Initial "hits" were retested and subjected to a dose-response assay at 1, 5, 10, and 25μM. Initially, 112 compounds scored as "hits." Of these, 21 compounds that reproducibly caused "strong reduction" in thymus fluorescence without obvious larval toxicity ≤ 10μM were retained for further evaluation.

Zebrafish embryo cell cycle analysis

Dechorionated embryos were incubated with compounds at 4 hours postfertilization (hpf). At 24 hpf, larvae were dissociated, stained with propidium iodide (PI), and analyzed for cell cycle status[38] using the ModFit LT Version 3.1 software (Verity Software House).

Leukemic zebrafish experiments

rag2. cMYC-ER zebrafish[22] were crossed with *lck*:EGFP zebrafish and leukemic adults were identified via fluorescence microscopy for T-ALL dissemination. Leukemic adults were treated either with vehicle or LDK on a 2-day-on, 1-day-off treatment regimen with daily water changes. Treatment was discontinued after 14 days. Tumor response was monitored twice weekly using the Olympus MVX10 Imaging System.

Tissue sections and staining

Fish were fixed in paraformaldehyde (4% in PBS), and sequential 4-micron-thick sections were either stained with H&E or with anti-GFP antibody (B-2; Santa Cruz Biotechnology) at 1:400 dilution with hematoxylin counterstaining.

Mouse xenograft experiments

Male nonobese diabetic (NOD)–severe combined immunodeficiency (SCID) mice were injected with 500 000 Matrigel (BD Bioscience) embedded CCRF-CEM-Luc cells per flank. After 3 days, mice were injected intraperitoneally twice daily with vehicle only (5% cremophor-EL, 5% N,N-dimethylacetamide, and 0.7% NaCl in ddH_2O at pH 6.0) or LDK (16 mg/kg) and monitored weekly for tumor progression using Xenogen IVIS 100 Imaging System (Caliper Life Sciences) and Living Image Version 2.50 software (Caliper Life Sciences). *P* values were calculated using Wilcoxon rank sum test.

Primary human leukemia samples

De-identified primary human patient samples were obtained under the University of Utah IRB protocol no. 10924. B-ALL samples (see Figure 5A-D) were cocultured with OP9 feeder cells. For CML specimens, frozen CD34$^+$ cells from peripheral blood (PB) of CML-CP (chronic phase) patients (n = 2) were cultured overnight in Iscove modified Dulbecco medium (IMDM) plus 30% FBS and 2mM L-glutamine supplemented with IL-3 (20 ng/mL), IL-6 (20 ng/mL), Flt-3 ligand (100 ng/mL), and kit ligand (100 ng/mL; StemCell Technologies). The CD34$^+$ fraction was isolated using the CD34 MultiSort kit (Miltenyi Biotec). For Ph$^+$ALL specimens, frozen mononuclear patient cells from PB were cultured overnight in IMDM plus 30% FBS and 2mM L-glutamine supplemented IL-7 (10 ng/mL; Peprotech) and treated as indicated.

Results

Zebrafish screen identifies compounds targeted to immature T cells

Our previous studies revealed that dexamethasone, known for its toxicity against human lymphoblasts, also eliminates immature T cells in the thymus of zebrafish larvae.[21] We reasoned that among the molecules identified in a drug screen for their activity against immature T cells in zebrafish, we would find novel compounds with the potential to eradicate human T-ALL cells. The use of the transgenic *lck*:EGFP line that fluorescently labels all T cells facilitates rapid assessment of a compound's effect on T-cell survival in a 96-well format by fluorescence microscopy.[21] Based on these considerations, 3 *lck*:EGFP transgenic zebrafish at 5 dpf were placed in each well of a 96-well plate and incubated for 2 days with compounds at 10μM from the ChemBridge DIVERSet library (Figure 1A-C). On retesting of 112 primary "hits" (among the 26 400 compounds screened) with strong reduction of EGFP-positive immature T cells in the thymus of zebrafish larvae, 21 were retained as candidates (supplemental Table 1, available on the *Blood* Web site; see the Supplemental Materials link at the top of the online article). To ascertain that these "hits," contrary to

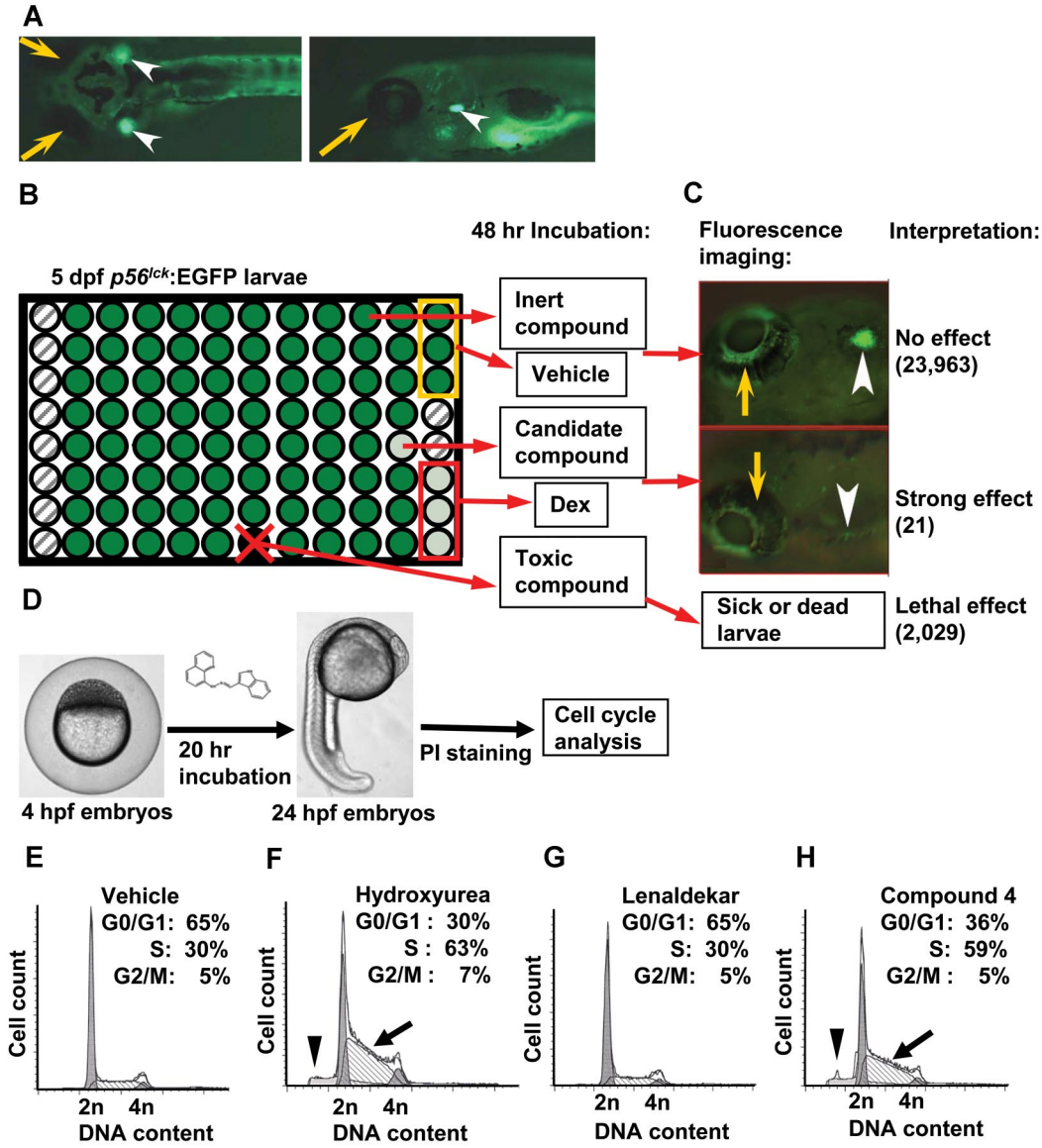

Figure 1. Zebrafish drug screen identifies anti–T-cell compounds. Zebrafish larvae carrying the T-cell specific *lck*:EGFP transgene were used for screening of a small molecule library for anti–T-cell effect. (A) Dorsal (left) and lateral (right) views of 5 days post fertilization (dpf) normal healthy *lck*:EGFP larva (yellow arrow indicates eye; and arrowhead, thymus). (B) Three 5-dpf larvae per well in 96-well format were treated with compounds, DMSO (vehicle, yellow box) and dexamethasone (Dex; positive control, red box). Fluorescence emission was evaluated after 48 hours: no effect/normal fluorescence (dark green), strong effect (light green), toxic effect (black well/red x), and empty well (hatched). (C) Examples of strong (bottom) and no effect (top). Of 26 400 compounds screened, 387 compounds with weak reduction of thymus fluorescence were also identified. (D) Twenty-one compounds with strong effect on survival of immature T cells were tested for cell cycle effects in nonlymphoid cells. Four hours postfertilization (hpf) zebrafish larvae were incubated in candidate compounds for 20 hours, dissociated into single-cell suspensions, stained with propidium iodide (PI) and subjected to flow cytometry. (E) Representative cell cycle profile for DMSO vehicle-treated embryos. (F) Hydroxyurea-treated embryos show S-phase arrest (arrow) as well as sub-G_1 peak (arrowhead). (G) Lenaldekar (5μM) shows a cell cycle profile similar to that of control embryos. (H) Compound 4 shows S-phase arrest (arrow) and sub-G_1 peak (arrowhead); 2n indicates G_0/G_1 phase; 4n, G_2/M phase; and between 2n and 4n, S phase. (A-C) Images were acquired at room temperature using Olympus MVX10 microscope with MV PLAPO 1× lens (Olympus). Camera used was Diagnostic Instruments model 14.2 Color Mosaic Insight FireWire SPOT. Acquisition software used was SPOT Alias Version 4.6 software, 2000 ms exposure with no binning, $\gamma = 1.0$. Fluorescence excitation light source was EXFO X-Cite Series 120. (D) Microscope used was Nikon Eclipse E600 with Nikon Plan APO 4× lens at room temperature. Camera used was CRI Nuance multispectral imaging system model N-MSI-420-FL. SPOT Advanced Version 4.6 acquisition software was used.

conventional chemotherapy, did not affect the cell cycle in all cell types, we incubated each with 20 zebrafish embryos at 4 hours postfertilization (hpf) and performed cell cycle analysis on cells isolated from whole embryos at 24 hpf (Figure 1D). Sixteen of the 21 compounds caused detectable cell cycle delays in S-phase or G_0/G_1 (supplemental Table 1) and some caused a sub-G_1 peak, indicative of cytotoxicity. The remaining 5 compounds had no effect on the cell cycle, caused no cytotoxicity (Figure 1E-H) and thus met criteria for drugs targeted to immature zebrafish T cells.

Lenaldekar induces apoptosis selectively in human leukemic blasts

Testing these 5 molecules by thiazolyl blue tetrazolium bromide (MTT) assay in the Jurkat T-ALL line (Figure 2A), one compound that we named LDK (Figure 2B) was the most potent with an IC_{50} consistently between 0.8 and −1.3μM, measured by both MTT (Figure 2A,D-F,H) and trypan blue exclusion test (Figure 2C). LDK was equally effective against the other 4 human T-ALL lines

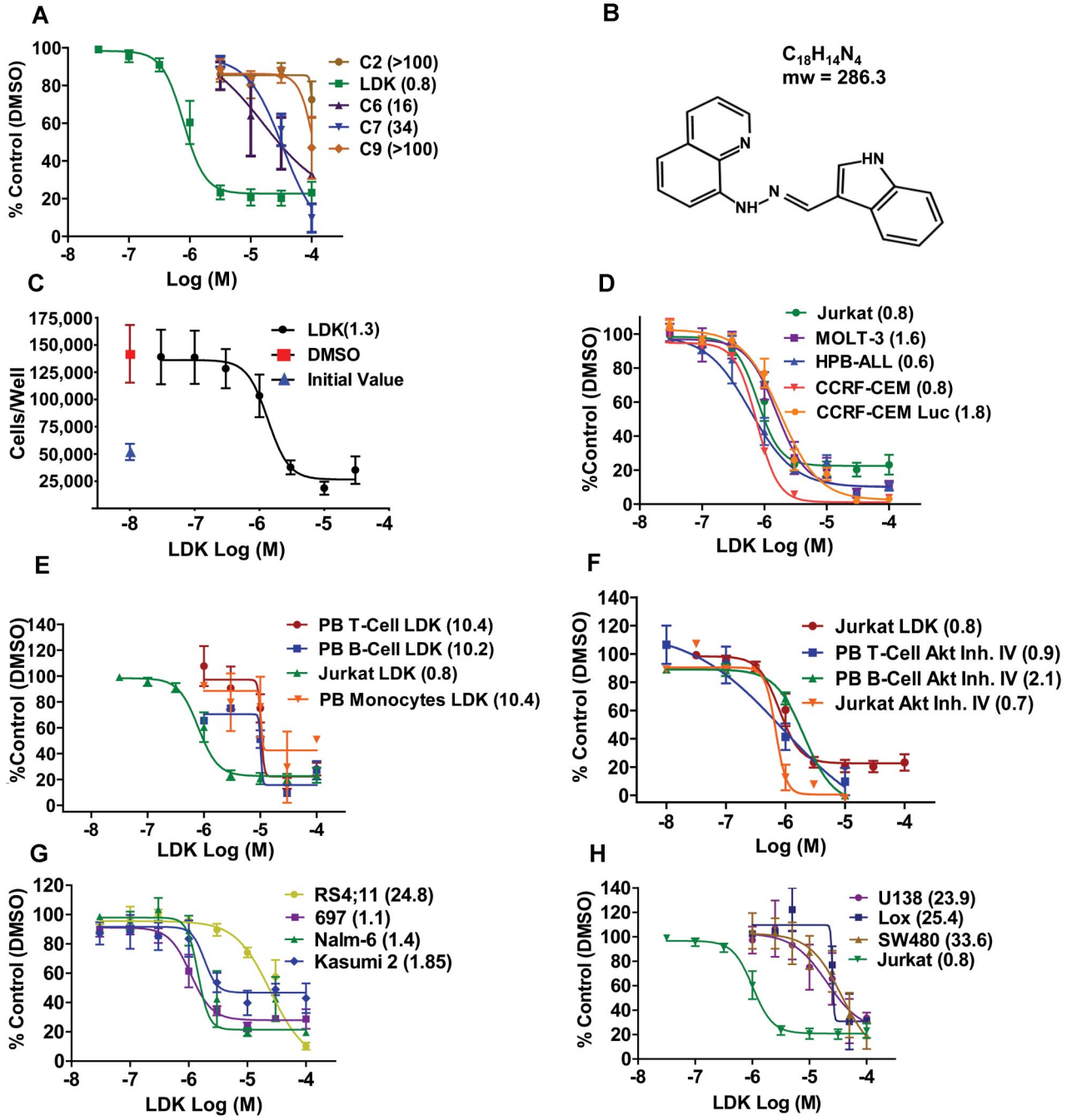

Figure 2. LDK is active against malignant lymphoblasts. IC_{50} values (μM) of indicated treatments by MTT assay after 48-hour incubation are shown in parentheses. (A) Among 5 hit compounds without general cell cycle effects, only Lenaldekar (LDK) had low micromolar activity against human Jurkat T-ALL (IC_{50} = 0.8μM). (B) LDK chemical structure (1H-indole-3-carbaldehyde quinolin-8-yl-hydrazone). (C) Trypan blue exclusion assay for LDK-treated Jurkat cells. (D) LDK dose-response for 5 human T-ALL lines. (E) LDK dose-response for PBTCs (stimulated with IL-2 30 U/mL), PB B cells (stimulated with IL-10 100 ng/mL), and PB monocytes from healthy human donors, compared with Jurkat. (F) Dose-response for LDK compared with AKT Inhibitor IV for Jurkat, PBTCs, and PB B cells. (G) LDK dose-response for 4 human B-ALL lines. (H) Jurkat T-ALL response to LDK in comparison to glioblastoma (U138), melanoma (Lox), and colon cancer (SW480). (A-H) n ≥ 3, error bars = SEM.

we tested (Figure 2D). LDK was more potent than GSI IX at inhibiting growth of 4 primary murine T-ALL lines harboring mutant NOTCH1, derived from *Atm*-deficient mice,[23] regardless of PTEN status (supplemental Figure 1). However, the IC_{50} of LDK in IL-2 stimulated peripheral blood T cells (PBTCs), B cells, and monocytes from healthy donors was 10-fold higher than in lymphoblasts (Figure 2E). AKT is an important enzyme in the survival of T-ALL cells and developing, immature thymocytes. We therefore chose an AKT inhibitor to test whether such a molecule would affect the survival of PBTCs. Interestingly, AKT inhibitor IV, equipotent to LDK against lymphoblastic cells, readily killed PBTCs (Figure 2F), which suggests that the lack of LDK activity against PBTCs was not based on general resistance to cell death in our assay system, and indicates a superior therapeutic window compared with a known AKT inhibitor. LDK was active against 3 B-ALL lines with an IC_{50} of 1 to 2μM, but higher concentrations (IC_{50} of ~ 25μM) were required against the RS4;11 line (Figure 2G). The IC_{50}s of 8 epithelial cancer cell lines tested ranged from

20 to 100μM, significantly higher than those for lymphoblastic lines, (Figure 2H, data not shown). To interrogate the apparent selectivity for lymphoid lineage malignancies, we tested LDK for efficacy against the NCI60 cell line panel. The 6 hematologic malignancy lines in this panel, including the multiple myeloma line RPMI-8226, the AML line HL-60, and the CML-derived line K-562, had IC_{50} values of 0.16 to 2.3μM, within the range of the T and B-ALL lines we had previously tested (supplemental Figure 2A). By contrast, the majority of the remaining 54 epithelial cancer lines had IC_{50} values more than 10-fold above the hematologic malignancy lines.

We next explored whether LDK killed Jurkat cells by apoptosis, the predominant form of cell death after drug treatment. Indeed, LDK at 1μM induced apoptosis in Jurkat cells, measured both by flow cytometry (supplemental Figure 2B), by Western blot (supplemental Figure 2C), and by activated caspase 3 staining (supplemental Figure 2D). LDK at 10μM caused only minimal visible toxicity in developing zebrafish embryos and larvae (supplemental Table 2).

LDK has in vivo activity in a zebrafish T-ALL model

We next tested whether LDK had anti–T-ALL activity in vivo. Affected adult individuals from the human cMYC-expressing line of zebrafish, crossed onto the *lck*:EGFP background (Figure 3A), were incubated with LDK at 250nM for 14 days on a 2-days-on/1-day-off treatment regimen. EGFP emission from T lymphoblasts was captured by fluorescence microscopy. Eighty-five percent of treated fish responded to LDK with a marked reduction of fluorescence extent and intensity (Figure 3B) and the remaining 15% of LDK-treated fish showed stable tumor burden (data not shown). To ascertain that fluorescence reduction was because of elimination of T-ALL cells, treated fish were sectioned and compared with untreated siblings. H&E staining of sections demonstrated a marked reduction in cells infiltrating nonlymphoid tissues such as skin and was mirrored by a decrease in EGFP-positive cells (Figure 3C) in treated individuals. This indicates that decrease in GFP intensity in LDK-treated zebrafish was because of absence of T lymphoblasts and not to quenching of the EGFP signal. By contrast, 100% of vehicle treated fish showed tumor progression and all succumbed to disease by day 40 (Figure 3B-D). Remarkably, despite the short course of treatment, the majority of LDK-treated fish maintained long-term remission (Figure 3D).

LDK is active against human T-ALL in murine xenografts

For in vivo efficacy testing in mammals, we intended to use luciferase-transduced Jurkat cells, but found that they did not engraft well into NOD/SCID mice (data not shown), as has been previously reported.[24] We therefore turned to luciferase-transduced CCRF-CEM T-ALL cells that had IC_{50} values (Figure 2D) similar to Jurkat cells, and engrafted better in NOD/SCID mice.[24] Other characteristics of CCRF-CEM cells were also similar to Jurkat cells (supplemental Figure 6). We embedded 5×10^5 cells in Matrigel and transplanted them into each flank of NOD/SCID mice.[25] Three days after xenografting, and then weekly for 4 weeks, mice were injected with luciferin and luminescence was measured. After the first measurement, mice were separated into 2 groups, one receiving diluent only, the other LDK at 16 mg/kg intraperitoneally twice daily. Luminescence was significantly lower in LDK-treated individuals on weeks 2, 3, and 4 (Figure 3E-F), resulting in a greater than 4-fold difference at the end of treatment. Furthermore, the average weight of the mice in each group was not statistically different at any time point, indicating lack of gastrointestinal toxicity of LDK (Figure 3G).

LDK leads to inhibition of the P/A/mT pathway

Next we wanted to identify the biologic pathway modulated by LDK. Our screening rationale predicted a pathway on which both immature developing T cells and developmentally arrested, immature T lymphoblasts are critically dependent. An obvious candidate is the P/A/mT pathway that is important for survival of immature T cells.[26] In addition, the recent detection of high-frequency abnormalities in the P/A/mT pathway in T-ALL[11] explains their exquisite sensitivity to inhibition of this pathway.[27] Western blot experiments showed that LDK, but not dexamethasone (data not shown), led to diminished phosphorylation of AKT on both T308 and S473 (Figure 4A). Similarly, LDK led to dephosphorylation of mTOR and of p70S6 kinase (S6K), a direct mTOR target (Figure 4B-C). Decreased AKT and mTOR phosphorylation was first detectable 1 hour after incubation with LDK at 2.5 and 5μM, respectively (supplemental Figure 3A), close to the IC_{50} in Jurkat cells. To determine the effects of LDK on AKT's phosphorylation dynamics, we examined LDK's ability to prevent serum-induced phosphorylation of serum-starved cells. Among T-ALL lines tested, CCRF-CEM showed the most robust decrease in AKT phosphorylation after 72 hours of serum starvation. The known PI3K inhibitor Ly294002 blocked any rephosphorylation of AKT with a 15- or 30-minute preincubation time (supplemental Figure 3B). LDK, on the other hand, did not block serum-induced AKT phosphorylation even after 30 minutes of preincubation and showed reduction of AKT phosphorylation first at 15 minutes after serum-stimulation (supplemental Figure 3B). We have also examined phosphorylation dynamics of S473 and have obtained identical results to T308 (data not shown).

To test whether P/A/mT pathway inhibition was selective and a general feature of LDK's activity in lymphoblastic cells, we assessed murine B-cell lines Ramos and BaF3 by Phosflow analysis.[28] Growth factor–independent Ramos cells have baseline hyperphosphorylated SRC and S6 ribosomal protein (S6; supplemental Figure 3C). As expected, the tyrosine kinase inhibitor dasatinib reduced SRC phosphorylation to background levels but did not affect S6 phosphorylation. Conversely, LDK did not affect pSRC but reduced S6 phosphorylation close to background levels (supplemental Figure 3C). The IL-3 dependent pro-B cell line BaF3 shows increased phosphorylation of signal transducer and activator of transcription (STAT)3 and S6 after IL-3 stimulation (supplemental Figure 3D). As expected, JAK Inhibitor I reduced IL-3–induced phosphorylation of both STAT3 and S6 to background levels. In contrast, LDK prevented IL-3–induced phosphorylation of S6 but not of STAT3 (supplemental Figure 3D). Furthermore, LDK did not affect IL-3–induced phosphorylation of STAT5, ERK1/2, or p38 in BaF3 cells (data not shown). These findings support selective action of LDK on the P/A/mT signaling pathway in lymphoblastic lines.

Next we wanted to determine whether inhibition of the P/A/mT pathway was required for LDK's cytotoxic activity. For this we modified a myristoylated form of AKT (myr-AKT, a kind gift from Dr S. Grant) that targets AKT to the plasma membrane, by introducing phosphomimetic aspartic acid residues at T308 and S473. We introduced this constitutively active form of AKT (myr-AKT-DD) into Jurkat cells. Expression and activity of the construct was demonstrated by Western blot (supplemental Figure 4A). Whereas native Jurkat cells responded to LDK treatment with PARP cleavage and marked decrease in viability, constitutively

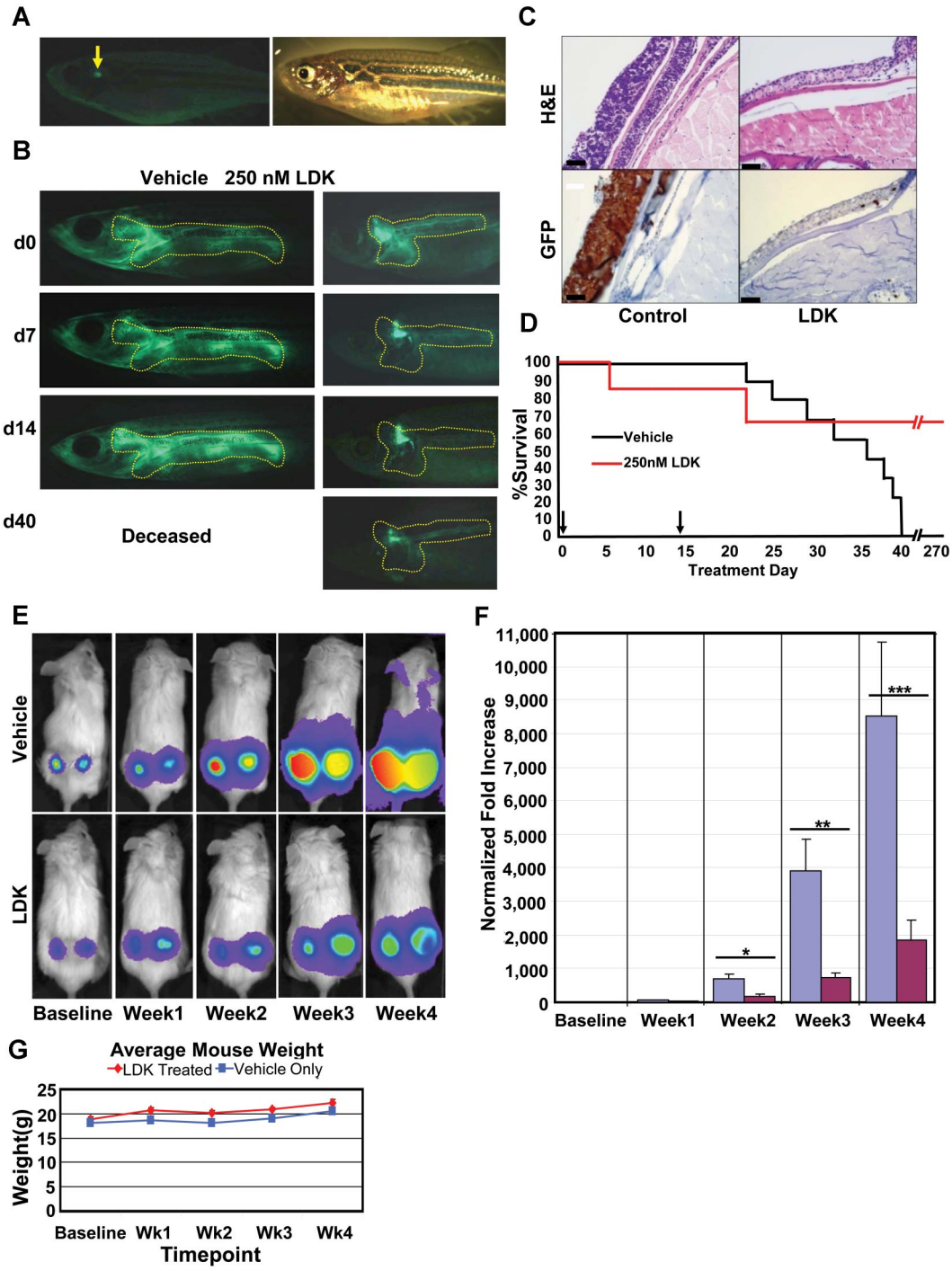

Figure 3. LDK treatment inhibits tumor progession in 2 in vivo models of T-ALL. (A-D) Adult *rag2*:cMYC-ER/*lck*:EGFP transgenic zebrafish with T-cell leukemia infiltration (outline) were treated with DMSO vehicle (n = 10) or 250nM LDK (n = 20) dissolved in E3 fish water over a 2-week period. As continuous exposure to LDK had toxic side effects, fish were subjected to a well-tolerated 2-day on drug/1-day off drug treatment regimen before being taken off drug altogether after day 14. (A) Fluorescence (left) and bright field (right) imaging of normal healthy adult *rag2*:cMYC-ER/*lck*:EGFP transgenic fish (arrow indicates normal T-cell fluorescence in thymus). (B) Treatment outcome of leukemic zebrafish incubated in DMSO vehicle only or 250nM LDK. One representative fish shown per treatment. (C) Vehicle control (left panels) and LDK treated (right panels) leukemic fish were sectioned and stained with H&E (top panels) as well as immunohistochemistry staining for GFP (bottom panels). Scale bars, 10 μm. (D) Kaplan-Meier survival plot shows superior survival of LDK-treated fish. Although all vehicle-treated fish (10/10) had expired by day 40, 67% of LDK-treated fish (13/20) were alive at day 270 (256 days after treatment). Three LDK-treated fish expired of unknown causes. Arrows indicate start and end time points of treatment. (E-G) LDK treatment inhibits tumor growth in a mouse xenograft model of T-ALL. Thirty male NOD-SCID mice were injected in each flank with 5×10^5 luciferase-transduced CCRF-CEM T-ALL cells. Cells were then allowed to engraft for 3 days before first bioluminescence measurement. The mice were then divided into 2 groups of 15 mice each and treated twice daily via intraperitoneal injection with either LDK (16 mg/kg) or vehicle only. Bioluminescence was assessed weekly with a CCD camera. (E) Representative pictures for tumor progression in vehicle control (top) versus LDK-treated (bottom) mice. (F) Increase in tumor bioluminescence of vehicle and LDK-treated mice, normalized to baseline. (*P = .0265, **P = .0006, ***P = .0304). (G) Average weight of LDK-treated (red line) versus vehicle only (blue line) treated mice. Error bars = SEM. (A-B) Images were acquired at room temperature using the Olympus MVX10 microscope with MV PLAPO 1× lens (Olympus). Camera used was Diagnostic Instruments model 14.2 Color Mosaic Insight FireWire SPOT. SPOT Alias Version 4.6 acquisition software was used, 2000 ms exposure with no binning, γ = 1.0. Fluorescence excitation light source was EXFO X-Cite Series 120. (C) Images were obtained using automated immunostainer (BenchMark XT; Ventana Medical Systems) followed by IView DAB detection (Ventana Medical Systems). (E) Mouse images and tumor emittance data were collected at 37°C using the XENOGEN IVIS 100 imaging system (Caliper Life Sciences) with Spectral Instruments 600 Series camera controller. Mouse images were processed and analyzed for quantitative emittance using Living Image Version 2.50.2 software (Caliper Life Sciences).

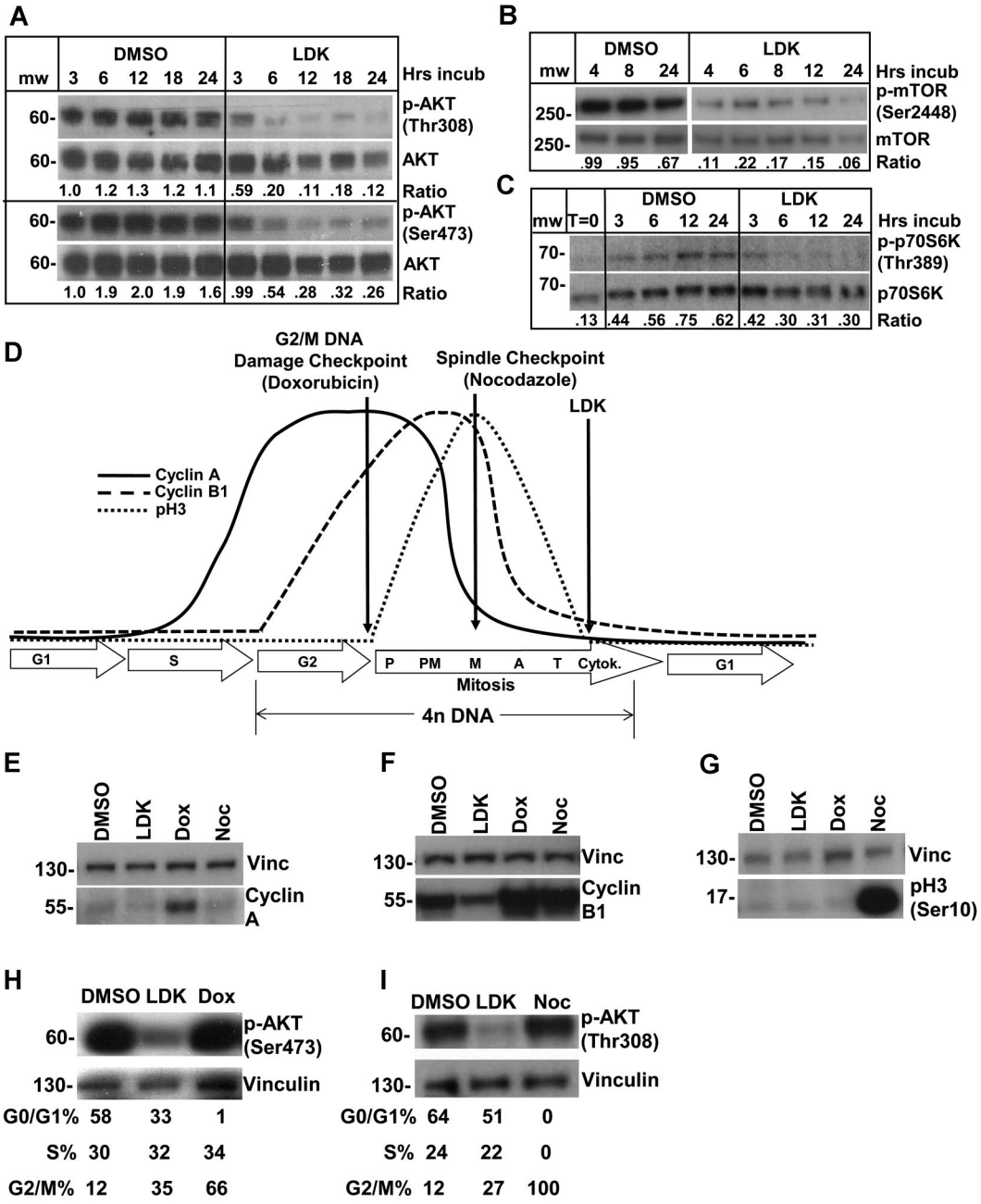

Figure 4. LDK down-regulates phosphorylation of targets in the PI3K/AKT/mTOR pathway and causes late mitosis arrest in treated cells. (A-C) Jurkat cells were treated with 10μM LDK for the indicated durations then probed for phospho as well as total proteins by Western blot. Densitometric ratio of phospho to total protein is indicated below the paired panels. (A) LDK treatment reduces phosphorylation of AKT at Thr308 and Ser473. (B) LDK treatment reduces phosphorylation of mTOR. (C) LDK treatment reduces serum-induced phosphorylation of mTOR downstream target, p70S6 kinase, at 6 hours of treatment. Note that LDK did not prevent serum-induced phosphorylation of p70S6K at 3 hours. (cropped, noncontiguous sections of same gels are shown for panels A-C). (D-G) Western blot assessment of LDK-treated Jurkat cells indicates that the G_2/M block occurs after anaphase. (D) Schematic of cyclin A and B1 as well as phospho-histone H3 (pH3) temporal expression patterns observed during the mammalian cell cycle. (E-G) Western blot assessment of LDK (10μM) treated cells indicates that neither cyclin A, cyclin B1, nor pH3 accumulate in treated cells. Treatment durations were 24 hours for E and 16 hours for panels F and G. Dox indicates100nM doxorubicin; Noc, 1μM nocodazolel; and dox and noc, positive control. (H-I) Western blot assessment of Jurkat cells treated with the inhibitors doxorubicin and nocodazole indicates that these inhibitors do not cause dephosphorylation of AKT. (E-I) Vinc indicates vinculin loading control, noncontiguous sections of same gel. Western blots were scanned at room temperature using Epson Expression 1680 scanner and software, 16-bit grayscale acquisition, 300 dpi resolution. Image processing was done using Adobe Photoshop 9.0.2.

active AKT caused almost complete inhibition of PARP cleavage and increased LDK's IC_{50} 3-fold (supplemental Figure 4A-C). Although these data suggest that inhibition of the P/A/mT pathway is at least partially required for LDK's cytotoxic activity in Jurkat cells it does not address whether LDK's action on the P/A/mT pathway is direct or indirect.

To answer this question, we sought to identify enzymes whose activity LDK may be modulating. Using purified protein substrates for in vitro kinase assays we tested 33 enzymes, including members of the P/A/mT pathway and serine/threonine and tyrosine kinases that may act on the P/A/mT pathway. Whereas the nonspecific kinase inhibitor staurosporine at 1μM potently inhibited the

majority of these enzymes, high doses of LDK (25μM) were required to achieve a mild (20%-30%) reduction in activity of 2 tyrosine and 2 serine/threonine kinases (supplemental Table 3), and inhibited the remainder of the tested enzymes less than 20%. To confirm these data we have also tested 451 different kinases, including lipid and atypical kinase families (KINOME*Scan*). Remarkably, LDK at 1μM did not inhibit any of the kinases to a significant degree ($< 35\%$ of control activity, data not shown). Taken together, these data suggest that unlike staurosporine, LDK is not a nonspecific kinase inhibitor. Rather, it potently induces inhibition of the P/A/mT pathway in lymphoblasts, probably by acting on an as of yet unidentified upstream target.

LDK induces cell cycle delay in late mitosis

In most cells, conventional P/A/mT inhibitors, such as wortmannin, delay the cell cycle in G_0/G_1 (supplemental Table 4). Surprisingly, in 4 LDK-sensitive (Ls) lines (Jurkat, CCRF-CEM, 697 and Nalm-6) LDK induced G_2/M delay, whereas the LDK-resistant (Lr) line RS4;11 was delayed in G_0/G_1 (supplemental Table 4). A time-course in Jurkat cells showed that G_2/M delay was detectable by 4 hours after LDK treatment (supplemental Figure 5), and subsequently cells progressively accumulated in G_2/M. To determine the specific timing of the LDK induced G_2/M delay, we analyzed the expression of cyclin A, cyclin B1, and phospho(Ser10)-histone H3 (pH3), whose levels are all highly regulated (Figure 4D) within the mammalian cell cycle.[29,30] Whereas the relative expression of these 3 proteins in Jurkat cells accurately described doxorubicin-induced G_2 delay and nocodazole-induced metaphase delay, LDK treatment showed a very different profile, indicating an accumulation of cells in late mitosis (Figure 4E-G).

Taken together our results suggest that LDK has 2 activities in Ls cells: indirect inhibition of the P/A/mT pathway and cell cycle delay in late mitosis. We asked whether these 2 activities are dependent on each other. As P/A/mT inhibition with wortmannin does not lead to mitosis delay in the T and B-ALL lines we tested (supplemental Table 4), we probed whether, conversely, G_2/M delay could cause reduced AKT phosphorylation. We induced G_2 delay with doxorubicin and mitosis delay using nocodazole. Neither G_2 nor M delay reduced phosphorylation of AKT in Jurkat cells (Figures 4H-I). We therefore conclude that LDK has 2 independent activities in Ls cells and that inhibition of the P/A/mT pathway is not a mere consequence of ill health of LDK-treated cells.

Favorable pharmacokinetics and lack of endorgan toxicity in LDK-treated mice

We tested serum concentrations of LDK after 14 days of twice daily intraperitoneal application of LDK at 16, 80, and 200 mg/kg. Serum concentrations, measured 24 hours after the last intraperitoneal LDK application, were proportional to the applied doses (supplemental Figure 7A-B). Determination of pharmacokinetic properties of LDK in mice revealed a plasma elimination half-life of ~ 2 hours after both single oral and intravenous administration (supplemental Figure 7C). In toxicology studies, mice were treated with LDK by gavage at doses up to 45 mg/kg for 14 days. Mice remained healthy, did not show weight loss even at the highest dose, and serum protein, renal, and liver function tests were not significantly influenced by LDK treatment, regardless of dose (data not shown). Pathologic examination of kidneys and livers of diluent and 45 mg/kg LDK-treated animals showed no toxic effects (supplemental Figure 7D). LDK-treated individuals showed no significant difference compared with diluent-only treated mice in PB counts, spleen, and thymus differential cell counts (supplemental Figure 8A-C). We observed a 10% drop in the percentage of CD8 single-positive T lymphocytes in the thymus that may be a reflection of the particular sensitivity of immature, intermediate, CD8 single-positive thymocytes to AKT inhibition.[31] Total numbers of thymocytes and overall size of thymi were reduced by approximately 50% (data not shown).

LDK kills the majority of primary human leukemia cells

To interrogate the clinical relevance of our data, we asked whether LDK had activity against primary human leukemia samples. We tested several primary B-ALL samples either grown directly in culture (supplemental Figure 9, supplemental Table 6) or on OP9 stromal cells (Figure 5A-D, supplemental Table 5) including treatment-refractory, relapsed BCR-ABL B-ALL and T315I-mutated BCR-ABL positive B-ALL samples. We found that proliferation was strongly inhibited in 85% of patient B-ALL samples and that they exhibited G_2/M delay, similar to Jurkat cells (Figure 5). As the NCI60 data indicated that LDK might have activity against CML, we also tested 2 primary samples from patients with imatinib-resistant CML, one with wild-type BCR-ABL, the other with the T315I mutation. Colony assays demonstrated strong activity of LDK against both samples, whereas high doses of imatinib had only mild effects (Figure 5E). Finally, we tested 3 primary imatinib-resistant Ph^+ B-ALL samples for viability in the presence of LDK (Figure 5F). Samples 11-008 and 11-032 are paired diagnosis and relapse samples, with the relapse sample showing decreased sensitivity to LDK treatment. By contrast, LDK did not compromise health of normal bone marrow mononuclear cells at concentrations up to 3μM (Figure 5G). Similarly, the IC_{50} of proliferating human CD34 positive cord blood cells was 8-fold higher than leukemia cells (Figure 5H), supporting LDK's therapeutic window we had observed with normal PB mononuclear cells (Figure 2E). In sum, LDK was active against the majority of primary human leukemia samples, and led to G_2/M delay in Ls cells.

Discussion

The screen described herein represents the first successful and unbiased approach using zebrafish larvae to identify molecules with potency against a human cancer from a small molecule library containing compounds with unknown activity. Zebrafish have been increasingly used to screen for bioactive compounds with possible clinical relevance. For example, a screen of 2000 well-characterized compounds (Spectrum Library, MicroSource Discovery System) revealed PGE2 as a stimulator of hematopoietic stem cell growth,[32] a finding that is now being translated into clinical trials (L. Zon, personal e-mail communication, December 13, 2011). In another screen of the Spectrum Library for active compounds in a zebrafish model of acute myeloid leukemia (AML), Yeh et al identified a new role for COX-2 and β-catenin in AML1-ETO–induced AML.[33] More recently, a screen of the Spectrum Library for chemical suppressors of neural crest development revealed a class of dihydroorotate dehydrogenase inhibitors that not only almost completely abrogate neural crest development in zebrafish but also markedly decrease melanoma growth both in vitro and in mouse xenograft studies.[34]

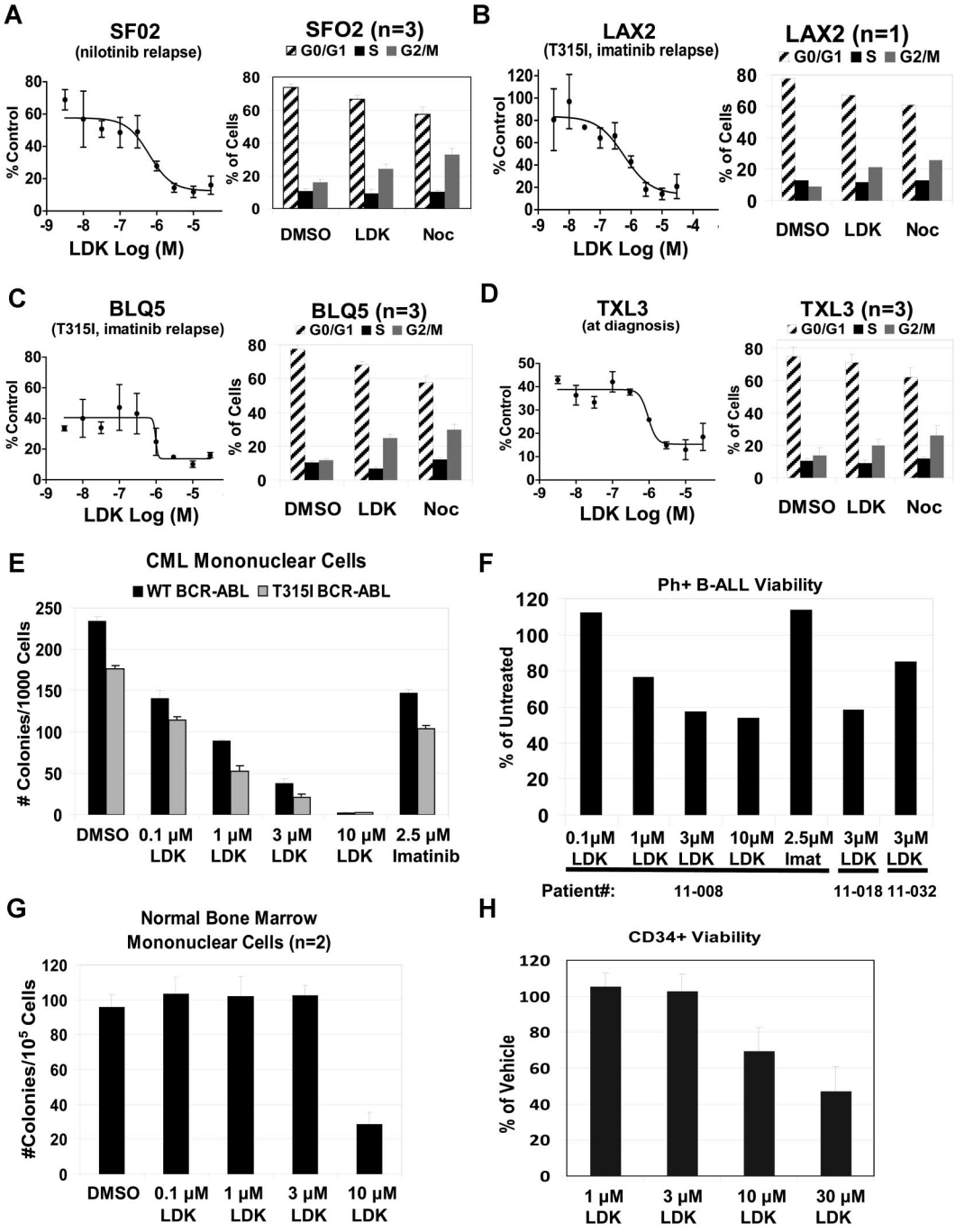

Figure 5. LDK is active against primary patient samples without toxicity to hematopoietic progenitors. (A-D) LDK decreases viability and induces G_2/M block in primary Ph^+ B-ALL patient samples. Left side of each panel shows MTT test of LDK dose-response viability assay at 48 hours incubation, n = 3, error bars = SD. Right side of each panel shows cell cycle profile for primary patient samples treated for 12 hours with DMSO, 10μM LDK, and 3μM nocodazole, n values as indicated, error bars = SEM. (E-H) LDK decreases viability of Ph^+ CML and B-ALL primary leukemias without toxicity to hematopoietic stem/progenitor cells (HSPCs). (E) Cytokine-dependent methylcellulose colony formation (mean ± SD) of CML-CP (CP indicates chronic phase) with wild-type BCR-ABL (patient ID no. 10-003, black bars) and T315I mutated BCR-ABL (patient ID no. 11-007, gray bars), either untreated or treated with the indicated inhibitors. (F) Trypan blue viability assay of mononuclear cells from 3 Ph^+ B-ALL patient samples treated with the indicated inhibitors. Samples 11-008 and 11-032 are paired samples from the same patient at diagnosis and relapse, respectively. (G) Cytokine-dependent methylcellulose colony formation (mean ± SD) of normal bone marrow mononuclear cells, treated with either DMSO or LDK at the indicated concentrations. (H) MTT viability assay of $CD34^+$ HSPCs from human cord blood, treated with LDK at the indicated concentrations, relative to vehicle control. Error bars = SD Additional primary patient sample characteristics may be found in supplemental Table 5.

Drug screening in zebrafish offers the obvious advantage of being conducted within the context of an entire vertebrate organism, including intact, heterologous cell-cell interactions (eg, thymocyte-thymic epithelial cells or hematopoietic stem cell–stromal cells). As our results demonstrate, such a screen can identify relatively nontoxic compounds with selective bioactivity in human cells. However, there are also clear limitations in how far we can extrapolate results from zebrafish drug screening to mammals. For example, zebrafish screens may have relevance for bioavailability as demonstrated by LDK. However, there are 3 routes of absorption

in fishes after immersion in compound (gastrointestinal, gill, and skin), compared with only one after oral application in mammals, and only the gill route is not available in zebrafish larvae at 5 dpf when we carried out the screen. In addition, the exposure to drug is constant and only restricted by stability in water during immersion, a different scenario from the intermittent oral dosing in mammals. Therefore, bioavailability in fishes may not accurately predict the same in mammals. Finally, targets may have diverged during evolution so that compounds that are active in zebrafish may not exhibit the desired effect in mammalian cells. This may be the case for the 4 compounds that had specific activity in zebrafish but did not kill Jurkat cells in our screen (Figure 2A).

Screening of large numbers of compounds is not practical in adult leukemic zebrafish. However, contrary to the AML model,[35] currently no zebrafish T-ALL models exist that manifest early in development to allow screening of thousands of compounds. We developed a 2-pronged screening strategy to identify targeted, nontoxic, antileukemia compounds in zebrafish larvae from a large chemical library. First, we reasoned that given their similar developmental stage, immature T cells and leukemic T lymphoblasts share similar pathways or biologic processes on which both critically depend. Consequently, compounds that eliminate the former may also kill the latter. Our rationale was supported by our previous finding that dexamethasone, a mainstay of anti-ALL treatment, eliminated immature T cells from the thymus of developing zebrafish larvae.[21] Our data that killing of immature zebrafish T cells and malignant human T-ALL lines by LDK involves indirect inhibition of the P/A/mT pathway (see below) bolstered our rationale as both types of cells critically depend on AKT activity for survival.[14,26,36] Second, we sought to identify active molecules that are devoid of general toxicity. The capacity to interfere with the cell cycle of dividing cells underpins the efficacy and toxicity of most chemotherapeutic agents. Despite species-specific variations, cell cycle regulation is highly conserved throughout metazoan evolution[37] and modulators of the cell cycle identified in zebrafish are active in mammals and vice versa.[38,39] We therefore reasoned that nontargeted compounds that are generally toxic to mammalian cells could be detected and eliminated by screening for cell cycle effects in developing zebrafish embryos (Figure 1D-H). Our finding that LDK has little toxicity in developing and adult zebrafish, mice, and nonmalignant human cells corroborates the rationale for our screening algorithm.

The P/A/mT pathway has become an attractive target for drug development[16] and molecules have been identified that inhibit 1[40,41] or 2[27,42,43] components of the pathway. The targets of these inhibitors are either the 3 enzymes themselves or kinases that activate the pathway, as for example PDK1[44] and mTORC2.[45] These inhibitors act against a wide range of tumor cell lines that depend on P/A/mT signaling.[46] LDK induces decreased phosphorylation state in members of the P/A/mT pathway and has potent activity against leukemias. Several lines of evidence indicate that LDK exerts an indirect effect on the P/A/mT pathway. First, extensive in vitro kinase assays clearly show that LDK does not significantly inhibit any of the members of the P/A/mT pathway. Second, in our serum starvation experiments, LDK exhibited markedly delayed activity on AKT phosphorylation compared with the PI3K inhibitor Ly294002. Third, LDK lacks activity against several AKT-dependent tumor lines, including glioblastoma and melanoma that are readily killed by AKT inhibitors. We therefore conclude that LDK's action on the P/A/mT pathway is indirect.

What is the underpinning of LDK's leukemia selectivity? Although the molecular basis of LDK resistance versus sensitivity remains the subject of future investigations, selective antileukemia activity could be explained by several mechanisms. These include a hematopoietic cell-restricted target (Figure 2, supplemental Figure 2), unique sensitivity of lymphocytes[47] to LDK's action, or differential drug metabolism by resistant versus sensitive lines.[48] Finally, the 2 activities of LDK may have to coincide for cytotoxicity. For example, hematopoietic cells can overcome cell cycle arrest in G_2/M through growth factor-stimulated activation of the P/A/mT pathway.[49] Thus, LDK's ability to induce G_2/M delay while simultaneously blocking the P/A/mT pathway, even after growth factor stimulation (supplemental Figure 3D), appears particularly significant. A requirement for dual activity is bolstered by our observation that in RS4;11 cells failure of LDK-mediated G_2/M delay correlates with resistance (Figure 2G, supplemental Table 4). We have shown that LDK's 2 activities, P/A/mT inhibition and late mitosis delay, are independent of each other (Figure 4H-I), but whether LDK accomplishes selectivity by interfering with single or multiple targets must be addressed in future studies.

In our study, LDK was active as monotherapy against all T-ALL lines tested and 85% of primary leukemia samples, regardless of PTEN status, resistance to glucocorticoids or other antileukemia compounds that may compromise patient treatment. Furthermore, with our dosing regimen LDK lacks endorgan (supplemental Figure 7D) and hematopoietic toxicity (Figures 2E and 5G-H, supplemental Figure 8). Thus LDK is an attractive, nontoxic compound that will form the basis of future endeavors to bring leukemia-selective treatments to the bedside.

Acknowledgments

The authors wish to acknowledge Ira Kraft, Jon Beck, Rupeng Zhuo, Kalavathy Ramachandran, and Bradley Demarest for expert technical assistance. Histology and immunohistochemistry were performed at the ARUP Institute for Clinical and Experimental Pathology with the technical assistance of Sheryl Tripp. Cell lines and fish strains were a kind gift of Joshua Schiffman, Randy Jensen, and Doug Grossman (University of Utah, Salt Lake City, UT); Adolfo Ferrando (Columbia University, New York, NY); and Andrew Kung, Alejandro Gutierrez, and Thomas Look (Dana-Farber Cancer Institute, Boston, MA). Dr Steven Grant (Virginia Commonwealth University Medical Center, Richmond, VA) provided the myr-AKT plasmid.

N.S.T. was supported by The Dana Foundation, The William Lawrence-Blanche Hughes Foundation, The Alex's Lemonade Stand Foundation, and the Huntsman Cancer Foundation. C.J.G. was supported by a grant from Genome Canada Competition III through the Ontario Genomics Institute. Core facilities of the Huntsman Cancer Institute, supported by National Cancer Institute grant P30 CA042014, and the University of Utah, supporting the CZAR zebrafish research core facility, also contributed to this work.

Authorship

Contribution: S.R., W.L.H., D.J., and N.S.T. conceived the experiments; H.C., P.C., H.S., A.S., E.J.M., and D.A.J. designed and carried out the zebrafish screen; D.A.J. carried out cell cycle analysis and toxicity studies on zebrafish embryos and larvae; D.A.J., W.L.H., and S.W. performed MTT assays, cell cycle, and antiactivated caspase 3 assay; K.B. and M.S. synthesized LDK; L.B. and J.K.F. conceived and carried out in vivo testing of LDK in

adult leukemic zebrafish; A.A., R.R.M., and G.J.S. carried out pathologic and biochemical evaluation of LDK-treated mice and zebrafish; J.E.C. developed the LC/MS assay to measure LDK concentrations; T.P., R.J., B.M., and C.J.G. conceived and performed Phosflow analysis, and efficacy testing of LDK in murine T-ALL lines and in primary human leukemias; A.E., M.M., M.D., and W.L.H. conceived and performed further experiments on primary human leukemia cells; and N.S.T. wrote the paper.

Conflict-of-interest disclosure: The authors declare no competing financial interests.

The current affiliation for M.M. is Department of Laboratory Medicine, University of California, San Francisco, San Francisco, CA 94143.

Correspondence: Nikolaus Sebastian Trede, The Huntsman Cancer Institute, University of Utah, 2000 Circle of Hope, Salt Lake City, UT 84112; e-mail: nikolaus.trede@hci.utah.edu.

References

1. National Cancer Institute, Surveillance Epidemiology and End Result. Stat Fact Sheets: Leukemia. Available at http://www.seer.cancer.gov/statfacts/html/leuks.html. Accessed December 10, 2011.
2. Smith MA, Gloeckler Ries LA, Gurney JG, Ross JA. Leukemia. SEER Pediatric Monograph. Available at seer.cancer.gov/publications/childhood/leukemia.pdf. National Cancer Institute. Accessed December 10, 2011.
3. Pui CH, Relling MV, Downing JR. Acute lymphoblastic leukemia. *N Engl J Med.* 2004;350(15):1535-1548.
4. Goldberg JM, Silverman LB, Levy DE, et al. Childhood T-cell acute lymphoblastic leukemia: the Dana-Farber Cancer Institute acute lymphoblastic leukemia consortium experience. *J Clin Oncol.* 2003;21(19):3616-3622.
5. Armstrong SA, Look AT. Molecular genetics of acute lymphoblastic leukemia. *J Clin Oncol.* 2005;23(26):6306-6315.
6. Ferrando AA, Look AT. Clinical implications of recurring chromosomal and associated molecular abnormalities in acute lymphoblastic leukemia. *Semin Hematol.* 2000;37(4):381-395.
7. Yeoh EJ, Ross ME, Shurtleff SA, et al. Classification, subtype discovery, and prediction of outcome in pediatric acute lymphoblastic leukemia by gene expression profiling. *Cancer Cell.* 2002;1(2):133-143.
8. Druker BJ, Tamura S, Buchdunger E, et al. Effects of a selective inhibitor of the Abl tyrosine kinase on the growth of Bcr-Abl positive cells. *Nat Med.* 1996;2(5):561-566.
9. Smith A. Screening for drug discovery: the leading question. *Nature.* 2002;418(6896):453-459.
10. Weng AP, Ferrando AA, Lee W, et al. Activating mutations of NOTCH1 in human T cell acute lymphoblastic leukemia. *Science.* 2004;306(5694):269-271.
11. Gutierrez A, Sanda T, Grebliunaite R, et al. High frequency of PTEN, PI3K, and AKT abnormalities in T-cell acute lymphoblastic leukemia. *Blood.* 2009;114(3):647-650.
12. Lai EC. Notch cleavage: Nicastrin helps Presenilin make the final cut. *Curr Biol.* 2002;12(6):R200-202.
13. Palomero T, Dominguez M, Ferrando AA. The role of the PTEN/AKT Pathway in NOTCH1-induced leukemia. *Cell Cycle.* 2008;7(8):965-970.
14. Palomero T, Sulis ML, Cortina M, et al. Mutational loss of PTEN induces resistance to NOTCH1 inhibition in T-cell leukemia. *Nat Med.* 2007;13(10):1203-1210.
15. Medyouf H, Gao X, Armstrong F, et al. Acute T-cell leukemias remain dependent on Notch signaling despite PTEN and INK4A/ARF loss. *Blood.* 2010;115(6):1175-1184.
16. Yap TA, Garrett MD, Walton MI, et al. Targeting the PI3K-AKT-mTOR pathway: progress, pitfalls, and promises. *Curr Opin Pharmacol.* 2008;8(4):393-412.
17. Cullion K, Draheim KM, Hermance N, et al. Targeting the Notch1 and mTOR pathways in a mouse T-ALL model. *Blood.* 2009;113(24):6172-6181.
18. Meeker ND, Trede NS. Immunology and zebrafish: spawning new models of human disease. *Dev Comp Immunol.* 2008;32(7):745-757.
19. Frazer JK, Meeker ND, Rudner L, et al. Heritable T-cell malignancy models established in a zebrafish phenotypic screen. *Leukemia.* 2009;23(10):1825-1835.
20. Langenau DM, Traver D, Ferrando AA, et al. Myc-induced T cell leukemia in transgenic zebrafish. *Science.* 2003;299(5608):887-890.
21. Langenau DM, Ferrando AA, Traver D, et al. In vivo tracking of T cell development, ablation, and engraftment in transgenic zebrafish. *Proc Natl Acad Sci U S A.* 2004;101(19):7369-7374.
22. Gutierrez A, Grebliunaite R, Feng H, et al. Pten mediates Myc oncogene dependence in a conditional zebrafish model of T cell acute lymphoblastic leukemia. *J Exp Med.* 2011;208(8):1595-1603.
23. Barlow C, Hirotsune S, Paylor R, et al. Atm-deficient mice: a paradigm of ataxia telangiectasia. *Cell.* 1996;86(1):159-171.
24. Fusetti L, Pruneri G, Gobbi A, et al. Human myeloid and lymphoid malignancies in the non-obese diabetic/severe combined immunodeficiency mouse model: frequency of apoptotic cells in solid tumors and efficiency and speed of engraftment correlate with vascular endothelial growth factor production. *Cancer Res.* 2000;60(9):2527-2534.
25. Masiero M, Minuzzo S, Pusceddu I, et al. Notch3-mediated regulation of MKP-1 levels promotes survival of T acute lymphoblastic leukemia cells. *Leukemia.* 2011;25(4):588-598.
26. Jones RG, Parsons M, Bonnard M, et al. Protein kinase B regulates T lymphocyte survival, nuclear factor kappaB activation, and Bcl-X(L) levels in vivo. *J Exp Med.* 2000;191(10):1721-1734.
27. Chiarini F, Fala F, Tazzari PL, et al. Dual inhibition of class IA phosphatidylinositol 3-kinase and mammalian target of rapamycin as a new therapeutic option for T-cell acute lymphoblastic leukemia. *Cancer Res.* 2009;69(8):3520-3528.
28. Sachs K, Perez O, Pe'er D, et al. Causal protein-signaling networks derived from multiparameter single-cell data. *Science.* 2005;308(5721):523-529.
29. McManus KJ, Hendzel MJ. The relationship between histone H3 phosphorylation and acetylation throughout the mammalian cell cycle. *Biochem Cell Biol.* 2006;84(4):640-657.
30. Morgan D. *The Cell Cycle.* London, United Kingdom: Oxford University Press; 2007.
31. Juntilla MM, Koretzky GA. Critical roles of the PI3K/Akt signaling pathway in T cell development. *Immunol Lett.* 2008;116(2):104-110.
32. North TE, Goessling W, Walkley CR, et al. Prostaglandin E2 regulates vertebrate haematopoietic stem cell homeostasis. *Nature.* 2007;447(7147):1007-1011.
33. Yeh JR, Munson KM, Elagib KE, et al. Discovering chemical modifiers of oncogene-regulated hematopoietic differentiation. *Nat Chem Biol.* 2009;5(4):236-243.
34. White RM, Cech J, Ratanasirintrawoot S, et al. DHODH modulates transcriptional elongation in the neural crest and melanoma. *Nature.* 2011;471(7339):518-522.
35. Yeh JR, Munson KM, Chao YL, et al. AML1-ETO reprograms hematopoietic cell fate by downregulating scl expression. *Development.* 2008;135(2):401-410.
36. Huo J, Xu S, Lam KP. Fas apoptosis inhibitory molecule regulates T cell receptor-mediated apoptosis of thymocytes by modulating Akt activation and Nur77 expression. *J Biol Chem.* 2010;285(16):11827-11835.
37. DePamphilis ML, Blow JJ, Ghosh S, et al. Regulating the licensing of DNA replication origins in metazoa. *Curr Opin Cell Biol.* 2006;18(3):231-239.
38. Murphey RD, Stern HM, Straub CT, et al. A chemical genetic screen for cell cycle inhibitors in zebrafish embryos. *Chem Biol Drug Des.* 2006;68(4):213-219.
39. Stern HM, Murphey RD, Shepard JL, et al. Small molecules that delay S phase suppress a zebrafish bmyb mutant. *Nat Chem Biol.* 2005;1(7):366-370.
40. Feldman RI, Wu JM, Polokoff MA, et al. Novel small molecule inhibitors of 3-phosphoinositide-dependent kinase-1. *J Biol Chem.* 2005;280(20):19867-19874.
41. Martelli AM, Tazzari PL, Tabellini G, et al. A new selective AKT pharmacological inhibitor reduces resistance to chemotherapeutic drugs, TRAIL, all-trans-retinoic acid, and ionizing radiation of human leukemia cells. *Leukemia.* 2003;17(9):1794-1805.
42. Fan QW, Knight ZA, Goldenberg DD, et al. A dual PI3 kinase/mTOR inhibitor reveals emergent efficacy in glioma. *Cancer Cell.* 2006;9(5):341-349.
43. Janes MR, Limon JJ, So L, et al. Effective and selective targeting of leukemia cells using a TORC1/2 kinase inhibitor. *Nat Med.* 2010;16(2):205-213.
44. Mora A, Komander D, van Aalten DM, et al. PDK1, the master regulator of AGC kinase signal transduction. *Semin Cell Dev Biol.* 2004;15(2):161-170.
45. Sarbassov DD, Guertin DA, Ali SM, et al. Phosphorylation and regulation of Akt/PKB by the rictor-mTOR complex. *Science.* 2005;307(5712):1098-1101.
46. Serra V, Markman B, Scaltriti M, et al. NVP-BEZ235, a dual PI3K/mTOR inhibitor, prevents PI3K signaling and inhibits the growth of cancer cells with activating PI3K mutations. *Cancer Res.* 2008;68(19):8022-8030.
47. Carson DA, Kaye J, Matsumoto S, et al. Biochemical basis for the enhanced toxicity of deoxyribonucleosides toward malignant human T cell lines. *Proc Natl Acad Sci U S A.* 1979;76(5):2430-2433.
48. Higgins CF. Multiple molecular mechanisms for multidrug resistance transporters. *Nature.* 2007;446(7137):749-757.
49. Henry MK, Lynch JT, Eapen AK, et al. DNA damage-induced cell-cycle arrest of hematopoietic cells is overridden by activation of the PI-3 kinase/Akt signaling pathway. *Blood.* 2001;98(3):834-841.